Effect of ClH aromatic substitution on structural and dielectric properties of poly(p-xylylene)

ARTICLE *in* POLYMER · JUNE 2012

Impact Factor: 3.56 · DOI: 10.1016/j.polymer.2012.05.016

4 AUTHORS:

Abdel Kahouli
National Graduate School of Engineering a…
36 PUBLICATIONS **122** CITATIONS
SEE PROFILE

Alain Sylvestre
University Joseph Fourier - Grenoble 1
124 PUBLICATIONS **795** CITATIONS
SEE PROFILE

Sébastien Pairis
French National Centre for Scientific Resea…
50 PUBLICATIONS **468** CITATIONS
SEE PROFILE

Jean-Francois Laithier
JCL Sàrl
8 PUBLICATIONS **17** CITATIONS
SEE PROFILE

Polymer 53 (2012) 3001–3007

Contents lists available at SciVerse ScienceDirect

Polymer

journal homepage: www.elsevier.com/locate/polymer

Effect of Cl_H aromatic substitution on structural and dielectric properties of poly(p-xylylene)

A. Kahouli [a,b,*], A. Sylvestre [b], S. Pairis [c], J.-F. Laithier [d]

[a] Grenoble Electrical Engineering Laboratory (G2ELab), Joseph Fourier University (UJF), CNRS, 25 Rue des Martyrs, BP 166, 38042 Grenoble Cedex 9, France
[b] Laboratory for Materials, Organization and Properties (LabMOP), Campus Universitaire-El Manar, 2092 Tunis, Tunisia
[c] Institut Néel 25 avenue des Martyrs bâtiment F BP 166, 38042 Grenoble cedex 9, France
[d] Comelec SA, Rue de la Paix 129 - CH-2301 La Chaux-de-Fonds, Switzerland

ARTICLE INFO

Article history:
Received 4 November 2011
Received in revised form
27 March 2012
Accepted 8 May 2012
Available online 15 May 2012

Keywords:
Dielectric study
Parylene families
Phase transition

ABSTRACT

A basic understanding of the structure–property relations and how they are influenced by the molecular architecture is imperative for the future development of polymer thin films in a large number of applications including those in the electronics industry. A new study has been illustrated in this work to demonstrate the effect of an aromatic Chlorine–Hydrogen substitution on the structural and dielectric properties of poly-para-xylylene (parylene N) ($(-CH_2-C_6H_6-CH_2-)_n$). X–Ray Diffraction (XRD) analysis reveals that the chlorination of the aromatic rings of poly-para-xylylene stabilize the crystalline structure of the materials (α–monoclinic), increases the d-spacing, decreases the crystallinity, and increases the value of the dielectric parameters. Furthermore, the permittivity is increased from 2.68 (PPX N) to 3.1 (PPX C) and the conductivity is increased by two order of magnitude at room temperature at frequency 1 KHz. Fourier Transformation Infrared Spectrometer (FTIR) and Energy Dispersion X-ray (EDX) analyses shows that the different as deposited parylene type are deprived of extrinsic polar bonds who can influenced on the dielectric properties. The increase of the dielectric properties and the changes of the morphologies structure are associated to the change in the intermolecular interaction due to the Cl_H aromatic substitution of poly-p-xylylene.

1. Introduction

Parylene N (also called poly-para-xylylene or PPX N) is the generic name for members of a unique family of thermoplastic semi–crystalline polymers that are deposited from cyclic dimer (di-p-xylylene) by the commercial Gorham method [1]. The name of parylene N, parylene C and parylene D refer specifically to the coatings produced from the Union Carbide Corporation dimers. PPX N is the reference material of the parylene families obtained from an unsubstituted cyclic ([2.2] para-cyclophane). Aromatic chlorination of the PPX N to different extents gives rise to parylene C (PPX C) and parylene D (PPX D) with one and two chlorine atoms on average per repeat unit (monomer), respectively. The chemical structure for various parylenes treated in this study is shown in Fig. 1.

These families of parylene are particularly adapted for the electronics industry [2] and medical [3–5] because of their inertness, gas phase deposition, pinholes free, conformal layers, excellent barrier properties, and room temperature deposition. Recently, a variety of microelectromechanical systems (MEMS) incorporating parylene was created [6,7]. They have also been incorporated as structural materials for microfluidic devices [8] and are being used successfully in electronics to provide enhanced reliability and a trouble-free life.

The impact of Halogen–Hydrogen substitution in the morphology structure and the molecular dynamics of polar polymers in comparison with analog non-polar polymers is one of the most interesting questions in this paper. The dielectric spectroscopy is a tool adapted particularly well to answer this question. So, after a comparative study of their chemical and physical properties, the molecular dynamics and the dielectric properties of these three polymers were then discussed based on this dielectric spectroscopy analysis in large frequency [10^{-4}–10^{6} Hz] and temperature [0–400 °C] ranges. The polar nature or not of these polymers and their particular crystalline characteristic confers, with each one of them, a specific dielectric answer more or less interesting for the application considered. Based on their chemical structure (Fig. 1),

* Corresponding author. Grenoble Electrical Engineering Laboratory (G2ELab), Joseph Fourier University (UJF), CNRS, 25 Rue des Martyrs, BP 166, 38042 Grenoble Cedex 9, France.
E-mail addresses: abdelkader.kahouli@grenoble.cnrs.fr, kahouli.kader@yahoo.fr (A. Kahouli).

0032-3861/$ – see front matter © 2012 Elsevier Ltd. All rights reserved.
doi:10.1016/j.polymer.2012.05.016

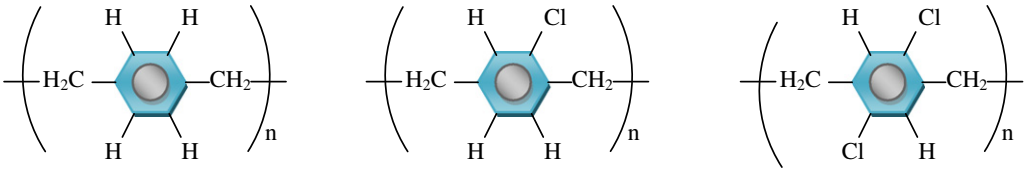

Fig. 1. Chemical structure of the most popular parylene families: parylene –N,–C and –D.

PPX N and PPX D appear as non-polar materials with the difference of PPX C. Indeed in this last, a strong dipole moment is attached to the aromatic ring in the main molecular chain. The polar character of PPX C is assigned mostly to the dipole orientation at low temperature and high frequency and by the cooperative mobility of polymeric chain at high temperature and low frequency [9].

In this work, the chemical and physical structure, real and imaginary parts of the complex permittivity and the electrical conductivity of polar (PPX C) and non-polar (PPX N, PPX D) are studied in relation to the aromatic Chlorine–Hydrogen (Cl_H) atom substitution.

2. Experimental

PPX N-C-D were processed by the Gorham method at Comelec SA. These materials are deposited on stainless which are in contact with the gas phase (vapor deposition polymerization, VDP) in the process of polymerization. The main attractive reason to deposit the parylene families lies in its large temperature deposition (Fig. 2) without catalyst elements making conformal and pure films (pinhole free).

The growth rate follows an exponential decreasing law with the substrate temperature:

$$Log(d) = \frac{k_1}{T_s} - k_2 \quad (1)$$

where d is the film thickness, T_s is the substrate temperature and k_1; k_2 are two constants.

The first step of the deposition process is the sublimation of the solid dimer at 120–180 °C. The second step is the pyrolysis of the two methylene–methylene bonds at 620–670 °C to yield the stable monomeric diradicals, para-xylylene (case of PPX N). This step results in practically 100% conversion of the dimer to monomer [10]. Finally, the gaseous monomers go through the deposition chamber, which is held at room temperature, or lower, and at pressure $P \sim 50$ mTorr or below. The cold trap at approximately –80 °C is used to collect the unreacted dimer before they enter in the mechanical pump and to prevent these residual species (Fig. 3) to contribute to the growing film. The

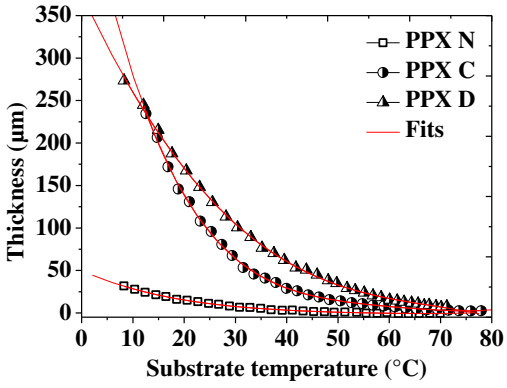

Fig. 2. Large temperature range of deposition parylene families.

measurement by Energy Dispersion X-ray spectroscopy (EDX) confirmed that the nature of these 'bubbles' (unreacted dimmer) are of the same nature as polymer deposited and not due to another impurities.

The parylene thicknesses are measured by reflectometry spectrometer (optical measurement). For dielectric measurements, top Au electrodes were deposited without heating the material using the evaporation method to constitute planar metal-insulator-metal (MIM) capacitors. Dielectric properties were measured using a Novocontrol BDS20 impedance meter in the frequency domain (10^{-4}–10^6 Hz) at temperature ranging from room temperature to 400 °C under 99.99% nitrogen gas. Chemical composition of PPX N, PPX C, and PPX D are studied by Fourier Transformation Infrared Spectrometer (FTIR), Nicolet 380 and by Energy Dispersion X-ray (EDX) analyses. Field effect scanning electronic microscopy (FESEM) Zeiss ultra plus is used to determine the morphology of the materials having 5.8 µm thick.

3. Result and discussion

Parylene families have sufficient properties which allow them to be used for many different applications in several domains due to the specificity of their spatial structure (Fig. 1). A phenyl group in the mainchain (as opposed to a side group as in polystyrene) enables the polymer to possess a higher thermal stability due to the aromatic higher bond strength and due to its ability to stabilize the adjacent bonds. However, the anisotropic molecular polarizability of benzene is $\Delta\alpha = 5.62$ Å^3. This anisotropy, which is evident in the repeating unit of the polymer, is also manifested in the real part of the complex permittivity of the polymer thin films.

In the most simplest sense, the PPX N repeat unit may be viewed as a phenyl group in series with two methyl groups (polyethylene) (Fig. 1) in which case the anisotropic molecular polarizability would be 5.62 and 0.721 Å^3 [11], respectively. Adding both values together yields 6.341 Å^3 for the addition of both segments (phenyl and polyethylene groups). The molecular polarizability increases from 0.65 (C–H) in PPX N to 2.61 (C–Cl) for PPX C and PPX D, and the dipolar moment increases from 0.4 Debye (C–H) to 1.46 Debye (C–Cl). It is well known that the real part of the complex permittivity is depending on the dipolar moment and the polarizability of the materials. Consequently, the real part of the complex permittivity in the case of PPX C and PPX D will be increases. The dielectric constant of the non-polar polymer is proportionally to the refractive index of the material, $\varepsilon = n^2$. Senkevich et *al* [11] have been more detailed the birefringence property in relation to the structure of PPX N, PPXC and PPX D. They are shown that the PPX N has a negative birefringence. As soon as substituted an hydrogen atom by a one (PPX C) or by two (PPX D) chlorine atom in the aromatic site, the birefringence becomes positive. From the study of Senkevich, we noted that ring-substituted chlorine changes totally the structure and the optic properties of the PPX N, consequently the dielectric constant. Before detailing the dielectric part, it would be necessary to understand the impact of Chlorine–Hydrogen (Cl_H) atom substitution on the chemical composition of the parylene families.

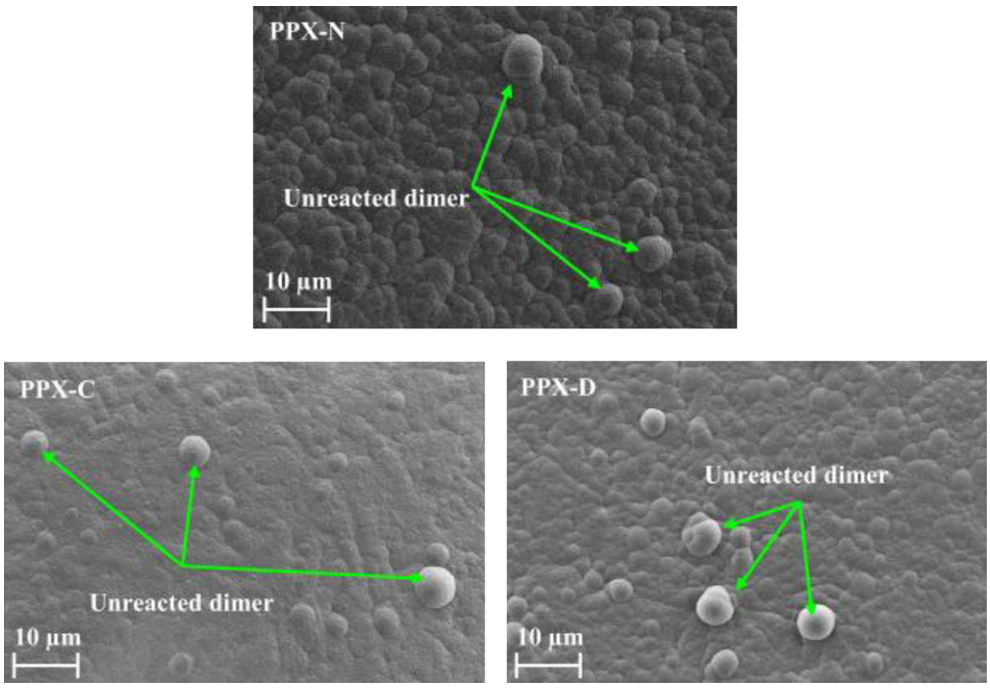

Fig. 3. Surface micrograph of parylene families analyzed by FESEM.

Fig. 4(a),(b) and Fig. 5 show the chemical composition of PPX N, PPX C and PPX D analyzed by FTIR and EDX, respectively. In this study we concentrate only at the two spectrum regions of the C–H stretching and the aromatic C–Cl bonds.

Some sets of peaks are very characteristic of PPX N in the 2800–3200 cm^{-1} bond region. The peaks are split into four because of the different C–H bonding which occurs in the PPX N mer unit but there are only three peaks for PPX C and PPX D (Fig. 4b). This behavior shows that the presence of the aromatic chlorine – hydrogen substitution remove an absorption peak (C–H bonds) in the case of PPX N which is replaced by one peak of C–Cl at 874.7 cm^{-1} for PPX C and by two C-Cl absorption peaks at 866.5 and 886.85 cm^{-1} for PPX D (see the gray area of Fig. 4(a)). The peak observed at 874.7 cm^{-1} in the case of PPX C migrates to the high wavenumbers (high energy) to wards 886.85 cm^{-1} (case of PPX D) is more intensive showing the increase in the intermolecular interaction. The increasing of the intermolecular interaction is due to the more electronegativity of the chlorine atom than the hydrogen atom. For this reasons, the presence of the chlorine atom in the parylene structure stabilize the rotation of the benzene rings due to the increase of the dipole–dipole interaction. In fact, in the presence of the high intensity of C-Cl in the PPX D, it correspond a low intensity peak of C–H aromatic observed at 815 cm^{-1}. This result is in good agreement with the number of the Cl_H substitution. When the number of the Hydrogen–Chlorine substitution increases, the intensity and the wavenumbers of C–Cl bonds increases and in the same way, the intensity and the position of the aromatic C–H bonds decrease (Fig. 4a). In the other hand, we can see in the EDX spectrum (Fig. 5) that the concentration (area of the peak) of the C–Cl bonds being very highest in the case of PPX D in comparison to PPX C (gray area in Fig. 5) while this peak is absent for PPX N. This result is consistent with its chemical structure (Fig. 1) and in good agreement with results obtained by FTIR analysis (Fig. 4).

It is interesting to noted also the absence of carbonyl bonds (C=O) and the carboxylic O–H impurities in the parylene films deposited by our VDP process. The presence of such elements in parylene composition can contribute on the polar character of the polymer and consequently, modify the dielectric properties.

Table 1 shows the impact of H–Cl aromatic substitution on the position of the C–H stretching bonds on the aliphatic and the aromatic sites of PPX N, PPX C and PPX D.

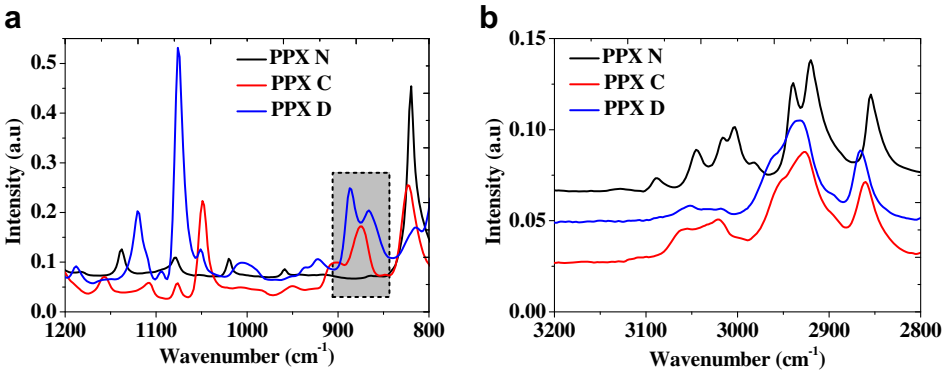

Fig. 4. FTIR analysis of the most popular parylenes, PPX N, PPXC and PPX D.

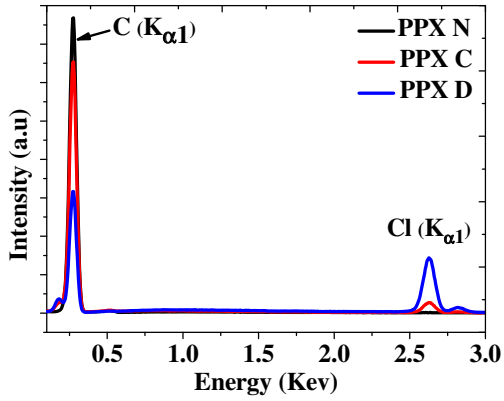

Fig. 5. EDX analysis of the most popular parylenes, PPX N, PPXC and PPX D.

Seeing to the chemical structure given in Fig. 1, Parylene N has a strong dipole symmetry described by the presence of C–H bonds with low electronic polarizability in the aliphatic sites. This chemical structure makes it a non polymer and facilitates the orientation and the arrangement of the macromolecular to constitute a polymer with high crystallinity ~60% [12] and with high molecular weight of about 2×10^5 [13]. These morphologies characteristic of PPX N allows it to have two structure transitions: one at 220 (α-monoclinic – β_1-hexagonal system (1)) and one at 270 °C (β_1-hexagonal (1) β_2-hexagonal (2) system) [13]. It was shown that the benzene rings of parylene-N below the first transition structure (α-monoclinic) are indeed oriented in the same direction and are parallel, which is preferentially oriented along the direction perpendicular to the substrate surface [040]. In the β-phase, the para-xylylene molecules are all parallel and oriented in the direction parallel to the substrates [200]. This last configuration presents a high birefringence according the study of senkevich et *al* [11]. The α-parylene N structure is the most stable thermodynamic form for films deposited near room temperature, but at low deposition temperature ($T < -60$ °C) and high deposition temperatures ($T > 80$ °C), β-polymorph is the more stable form. The polymer loses order along the direction of the chains above 270 °C and becomes a two-dimensional crystal with planar zigzag ordered sequence [13]. We can also obtain the β-form by annealing the film at a temperature of about 220 °C (Fig. 6). However, the crystalline phase undergoes further modifications before reaching its melting point of 420 °C [10] when heating the sample above 220 °C. This form was originally thought to be irreversible.

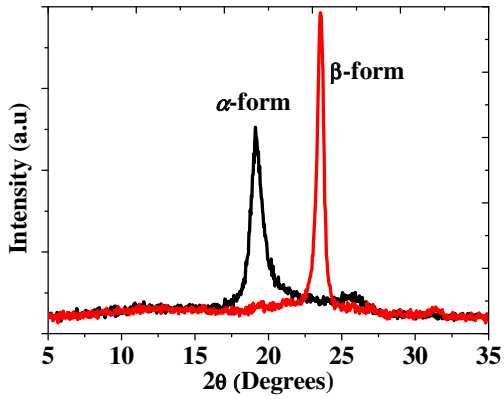

Fig. 6. XRD pattern of PPX N. Peak at low 2θ value is present. It is the (020) diffraction plane of the monoclinic unit cell (as deposited) and the large peak at higher 2θ value is from the (400) diffraction plane of the hexagonal unit cell obtained after annealing @ 220 °C for 10 min.

One ring substituted hydrogen-chlorine, gives the parylene C with a dissymmetric chemical structure (Fig. 1) due to the presence of a strong dipole moment (C–Cl). This type of parylene shows a single crystalline form very similar to the α–form of parylene N but the plan of the aromatic rings presents some inclination to the substrate [14]. Two ring substituted chlorine, gives the parylene D with α-monoclinic form. In the best of our knowledge, there is not a detailed crystal structure or molecular orientation on this film. Table 1

More structural information relating to the parylene families films versus the Cl_H substitution is given in Fig. 7, XRD spectrum from $2\theta = 4°$ to $2\theta = 36°$.

XRD characteristic may indicates the crystal disorder (crystallinity ratio), crystallite size for the thin films in terms of the full width half max (FWHM), d–spacing, and peak height of the diffraction planes. The diffraction peak observed between $2\theta = 12$ and 24° (Fig. 7) is attributed to the crystallographic system of the crystalline form presented in our parylene films deposited at room temperature. Table 2 summarizes the XRD data for PPX N, PPX C and PPX D homopolymer and the impact of Cl_H substitution on the structure development. As can be seen, the PPX exhibits an increase in d-spacing as it undergoes a substituted of an hydrogen atom by Chlorine, my be explained by the replacing of a small atom (Hydrogen) by a large atom (Chlorine) who requires a larger space to incorporated in the interchaine sites. The full width half max (FWHM) increases as the interchaine spaces increases due to the chlorine incorporation in the structure. This corresponds well to large decreases in the percent crystallinity and a decrease in the peak height of the (020) diffraction plane (Table 2).

The difference in the structure between the parylene families can be related to the deposition temperature of the material below or above T_g. The FWHM is large in the as deposited films below T_g owing to the presence of small crystallites and a high degree of crystalline disorder present within the PPXC (Tg ~ 90 °C) [6] and PPX D (Tg ~ 100 °C) thin films. Deposition temperature film above T_g (case of PPX N, Tg ~ 13 °C [15]) leads to smaller FWHM values because of more thermal energy available for crystallization resulting in larger more ordered polymer crystallites. This is in good agreement with the crystallinity ratio calculating by the Sherrer formula [16], (Table 2). However, why should such structural differences exist for poly-p-xylylene as a function of deposition temperature according the T_g or a function of Cl_H substitution? The answer may be the glass transition temperature which, according to the temperature deposition, is below or above. Vapor deposition polymerization (VDP) above the polymer's *Tg* can easily result in polymer crystallization. As the deposition temperature is above the *Tg* a greater degree of crystallization should take place. Most significant, PPX N has a *Tg* ~ 13 °C which is below room temperature, much different then either PPX C (80 °C) or PPX D (100 °C) which have *Tg*'s both above room temperature. It is evident that the presence of a bulkier atom as a pendent space attached to the main chain reduces the crystallinity and changes the growing mechanism, consequently, the molecular structure. However, PPX N show a crystallographic phase change α (monoclinic) to β (hexagonal) starting at 220 °C but remain unchanged in the either PPX C and PPX D (α-monoclinic form). The Cl_H substitution can be at the origin of such stabilizing of the physical structure of PPX C and PPX D. In

Table 1
C–H stretching and the aromatic C–Cl bonds of the most popular parylenes, PPX N, PPX C and PPX D.

Sample	C–H aliphatic				C–H aromatic			
PPX N	819	2854.3	2919.8	2939	3002.7	3016	3045	3087
PPX C	822	2860	2925.6	2950	–	3020	3058	–
PPX D	815	2865.4	2931.4	2960	–	3018	3050	–

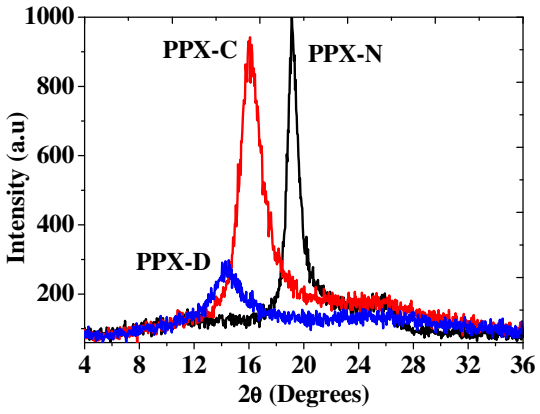

Fig. 7. XRD pattern of the most popular parylenes N, C, D.

fact, the high crystallinity of the PPX N is correlated to the deposition temperature which takes place above its T_g.

The morphology in turn affects the physical properties of the polymer thin film such as its elastic modulus, optical properties [14], and electrical properties such as its dielectric permittivity and losses.

The frequency and the temperature dependence of the complex permittivity are given by the equation.

$$\varepsilon^*\left(T,\omega\right) = \varepsilon'\left(T,\omega\right) - i\varepsilon''\left(T,\omega\right), \tag{2}$$

where ε' and ε'' are the real and imaginary parts of the complex permittivity, respectively. For polymer materials, the dielectric constant (real part of the complex permittivity), ε', is composed of four components as shown in Eq. (3):

$$\varepsilon' = \varepsilon_{\text{electronic}} + \varepsilon_{\text{ionic}} + \varepsilon_{\text{orientational}} + \varepsilon_{\text{interfacial}} \tag{3}$$

At optical frequency, the refractive index n is related to the real part of the complex permittivity by the Maxwell equation $\varepsilon' = n^2$. So, only the electrons can follow the variation of the applied field and consequently the only contribution to the dielectric constant should be from electronic phenomena. Therefore, Eq. (3) can be simplified as follows

$$\varepsilon' = \varepsilon_{\text{electronic}} \tag{4}$$

For non-polar materials, assuming that the absorption is negligible we can apply this relation in the frequency of our window measurement because for this type of materials the permittivity is governed by the electronic polarizability and is independent of frequency. For PPX N films with 2.68 at 1 KHz (Fig. 8(a)) of the real part of permittivity, the refractive index determined by spectroscopic ellipsometry were 1.66 [17]. This leads to a calculated $\varepsilon_{\text{electronic}}$ of approximately 2.75. The high proportion of $\varepsilon_{\text{electronic}}$ (~97.5%) to the total ε' indicates that contributions from $\varepsilon_{\text{ionic}}$, $\varepsilon_{\text{orientational}}$ and $\varepsilon_{\text{interfacial}}$ are very low and we can neglect them. However for PPX N, at kHz, there are more contributions to dielectric response. Therefore, one expects the kHz dielectric constant to be larger than the optical dielectric constant. The discrepancy may be related to the negligible of the optical absorption since $\varepsilon' = n^2 - \kappa^2$, where n is the refractive index and κ is a measure of optical extinction/absorption.

The PPXN is deposited as a partially opaque (dense) material from a few microns thick and the thickness of the material used for the dielectric measurement in our work is 5.8 μm. This optical property of PPX N can show some contribution of the absorption coefficient on the computed of the dielectric constant from the Maxwell equation. In a future study it should be makes measurement of the optical properties of PPXN to refine the relations between the optical and the dielectric properties.

Fig. 8(a) shows the variation of the dielectric constant, ε', with frequency at room temperature for all three poly(p-xylylene) films. The dielectric constant at 1 KHz is 2.68, 2.82 and 3.1 for the PPX N, PPX D and PPX C films, respectively. These dielectric parameters are slightly higher than those of conventional polymers including polyethylene, PE (2.25), polypropylene, PP (2.2) and polystyrene, PS (2.4) [18] which constituted essentially by only C–C, C=C and C–H bonds in the main chains. The difference in dielectric constant of these polymers in comparison with parylene families is due to the presence of benzene rings in the main chains of parylene associated to higher polarizability than the other chemical bonds. Fig. 8(a) also indicates a gradual decrease of the dielectric constant with increasing frequency after an initial sharp drop at low frequency for PPXD and strong relative permittivity dispersion for PPX C. This dielectric dispersion is associated to the polar character of PPX C due to the presence of a highly dipolar moment (C–Cl) in the structure. Kahouli et *al* [6] have detailed the dielectric response of PPX C in a large temperatures and frequencies range. Similar to the non-polar PPX N films, the dielectric constant of the PPX D films is mainly determined by the electronic polarization. The measured dielectric constant of 2.8 at 1 MHz is shown in Fig. 8(a) and the measured refractive index n of PPX D is approximately 1.67 [13]. The calculated value of $\varepsilon_{\text{electronic}}$ by the Maxwell's equation is 2.78 indicating that the major contribution to the total dielectric constant ε' is from the electronic polarization (~99%). Unlike the dielectric constant of conventional linear PPX D polymers which do not show significant frequency dependence due to, there is a distinct frequency dependence of the dielectric constant for PPX C films due to the asymmetric of its chemical structure. The higher real part of permittivity of PPX C (in comparison with PPX D and PPX N) is related to the strong polar character of the material due to the dissymmetric chemical structure of the monomer unit.

From comparison of the dielectric response measured at room temperature and in a large frequency region, it can be concluded that, regardless of the chlorine–hydrogen substitution, the ε' of PPX N and PPX D is practically independent of the frequency (Fig. 8(a)). The ε' measured at room temperature increases with increasing polarizability of the material. The difference in the frequency dependence of ε' observed on PPX N, PPX C and PPX D can be explained by the polar character of the materials. In polar materials, the dispersion phenomena observed at low frequency is mostly due to dipole orientation while in non-polar materials; only deformation of the electron shell is at the origin of the dielectric constant.

Fig. 9(a) and (b) show the temperature dependence of the real and the imaginary parts of the complex permittivity at 1 kHz. It can be seen that for PPX D, ε' is temperature independent with increasing temperature, with only the exception of a transient decline around T_g (100 °C). After 100 °C, ε' stabilize while the loss factor is temperature dependence. In contrast, to PPX N and PPX D, a dispersion of ε' is observed for PPX C with temperature (Fig. 9(a)) showing the polar character of this material. This behavior is mainly expressed by the appearance of a two peaks in the loss factor (Fig. 8(b)) associated to the C–Cl reorientation

Table 2
The main structure properties of PPX N, PPX C and PPX D as deposited films.

Sample	$2\theta_{\max}$ (°C)	d_{hkl}(Å)	$I_{\max}$ (cps)	FWHM (°)	Crystallinity (%)	Grain size (Å)
PPX N	19.16	5.37	39.6	0.90	60	104
PPX C	16.00	6.39	36.9	1.74	45	54
PPX D	14.52	7.08	11.9	2.02	39	46

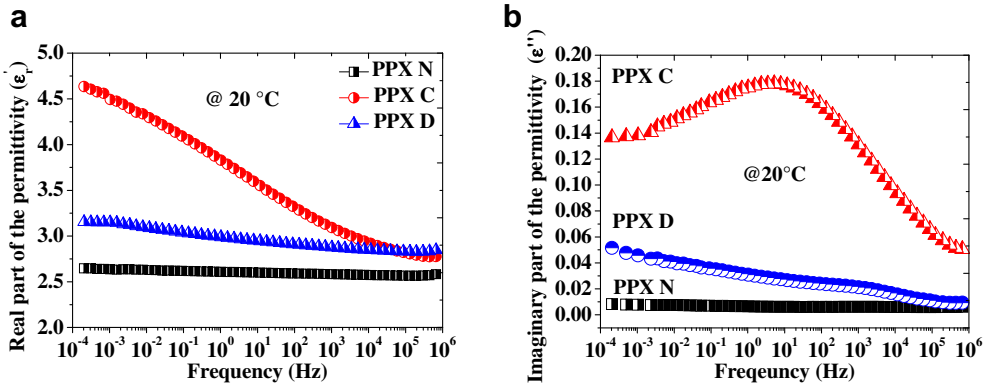

Fig. 8. Frequency dependence of the (a) real part and (b) imaginary part of the complex permittivity at room temperature for parylene families.

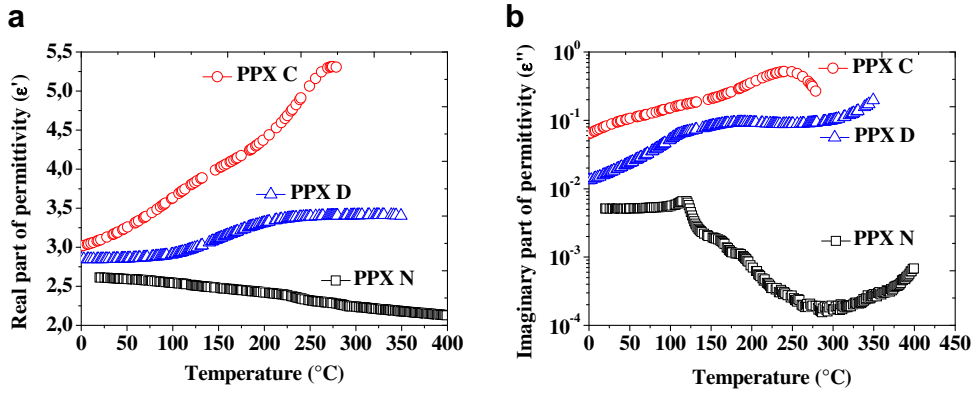

Fig. 9. Temperatures dependence of the (a) real part and (b) imaginary part of the permittivity at 1 KHz for parylene families.

(β−relaxation) and to the cooperative main chain motion (α-relaxation) [6], respectively as the temperature increases.

ε'', is an important parameters to characterize the dielectric loss, since it indicates the dissipation energy in the dielectric material due to the exponential decay of polarization with time once the applied field is removed. The measured dielectric losses at 1 kHz is ranging from 0.08 (PPX C) to 8 x 10^{-3} (PPX N) and 2.25 x 10^{-2} for PPX D as seen in Fig. 9(b).

As the temperature increases up to 400 °C, the ε' of PPX N is practically independent of the temperature and the loss factor is more rapid decreases of one decades from (5 x 10^{-3}) at 100 °C to (5 x 10^{-4}) at 220 °C and then increases above 270 °C. The increase of the PPX N losses above 270 °C is related to the phase transition of the material from β_1-hexagonal to β_2-hexagonal. The last structure form is more conductive than the others form (α-monoclinic and β_1-hexagonal) in PPX N. Furthermore, the electrical transport mechanism can be also studied directly from the conductivity analysis. The real part of the complex conductivity ranging from 220 to 380 °C is presented in Fig. 10. It can be seen that from 220 °C, the conductivity exhibit two different conduction regimes: A plateau at the low frequencies associated to the dc conductivity that bends off to a frequency dependent (Jonscher law) behavior at a critical frequency named ω_c (crossover frequency).

The value of the dc conductivity (σ_{dc}) for each isotherm varying between 220 and 380 °C can be taken from the plateau in the conductivity (Fig. 10(a)) curves. This value decreases with the

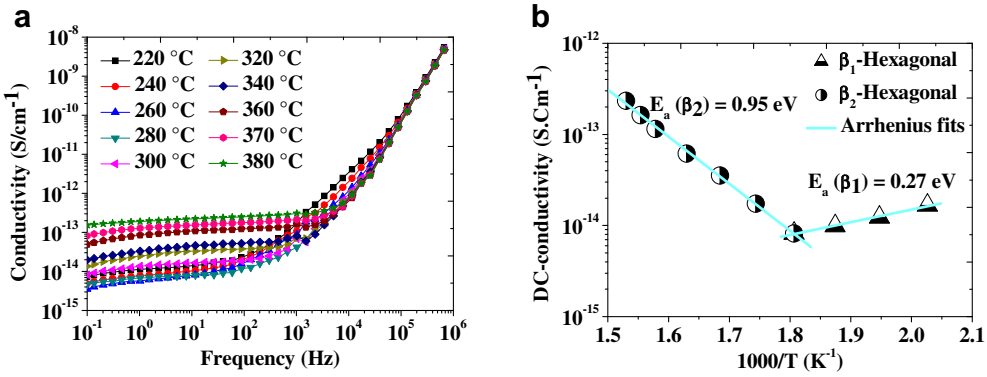

Fig. 10. Frequency dependence of the (a) electrical conductivity and (b) the activation energy of β1-hexagonal and β2-hexagonal for PPX N.

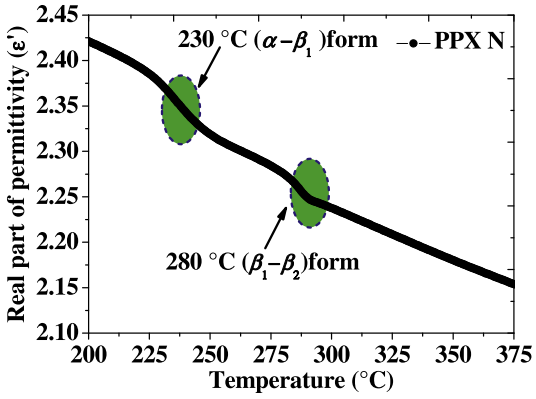

Fig. 11. Regions transition of PPX N deduced from the temperatures dependence of the real part of the permittivity at 1 KHz for PPX N.

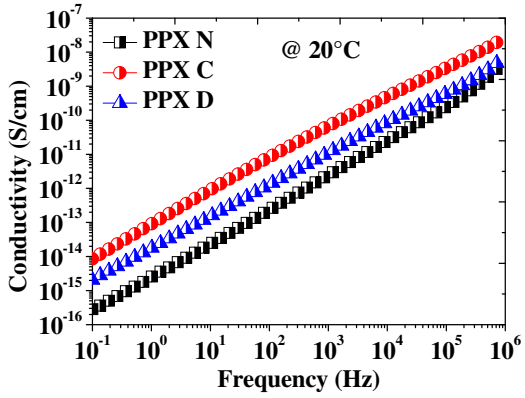

Fig. 12. Electrical conductivity according the frequency of parylene families.

temperature increase from 220 to 280 °C and it increases just after 280 °C with when the temperature increases. The representation of the dc conductivity in the activation plot (see Fig. 10(b)) clearly shows an Arrhenius behavior according the inverse of the measured temperature. The discontinuity in the values of σ_{dc} observed at temperature around 280 °C is due to the structure transformation occurring in the PPX N from β_1-hexagonal to β_2-hexagonal. The low conductivity of the parylene family may be due to the presence of only a small number of free charge carriers that have a small mobility. These carriers may be ions or electrons or originate from the dissociation of the dimer species observed by the FESEM (Field Effect Scanning Electronic Microscopy) at the parylenes surface (Fig. 3).

It was suggested that conduction below the transition temperature from β_1–hexagonal to β_2–hexagonal is predominately by electronic mechanism. In the β_1–hexagonal form of PPX N, the transport mechanism is being by jumps of the carriers from one side to another across a potential barrier of 0.27 eV (shallow trap). As the temperature increases and especially beyond the transition temperature (~280 °C), the conductivity exhibits a little dependence till the ionic contribution becomes significant at high temperature and the high potential barrier is about 0.95 eV (deep trap). In the some way, the plot of the variation of the permittivity according the temperature for the PPX N shows the presence of the different transition structure [Fig. 11(a)] as discussed previously.

The Cl–H aromatic substitution effect on the conductivity of PPX N at room temperature is illustrated on the Fig. 12.

It is evident seen from the plot that the conductivity of parylene increases with the substitution numbers of Cl–H., Since PPX C is the polar parylene, it presented the highly conductivity modulated by two order greater than the unsubstituted parylene (PPX N) at 0.1 Hz. The PPX D with the two symmetric chlorine atoms exhibit a conductivity between PPX N and PPX C. Due to the presence of two (C–Cl) bonds with a polarizability greater than the C–H in the case of the PPXC N and one C-Cl bond in the case of PPX C, PPX D has a conductivity value limited by the minimum conductivity of a non-polar material (PPX N) and a maximum conductivity of a strong polar material (PPX C). These modifications in the dielectric properties are due to the changes in the structure properties of parylene associated to the manner distribution of the chlorine atom in the aromatic sites of the monomer units.

4. Conclusion

Parylene materials deposited by chemical vapor deposition (CVD) under the optimum conditions from the same precursor family exhibit different structure–properties relations according to the Cl_H aromatic substitution. These materials exhibit a light increase in the dielectric constant than the corresponding conventional polymer materials (PE, PP, and PS). The bulk dielectric response is a structure origin in mainly. The small sharp drop in ε' at low frequencies can primarily be attributed to some orientational polarization caused by the presence of polar C–Cl groups. The measured dielectric loss is comparable to many conventional polymers materials at 1 kHz. It appears that the C–Cl polar content plays a dominant part in affecting the structure changes and the frequency dependences of both ε' and ε'' for the PPX C and PPX D films. The absence of the polar bonds C–Cl in the parylène N caused a polymorphism structure assigned by the presence of three crystalline systems while a homomorphism structure in the case of PPX C and PPX D with the presence of the C–Cl bonds.

References

[1] Gorham WF. J Polym Sci A-1 1966;4:3027–39.
[2] Jakabovič J, Kováč J, Weis M, Haško D, Srnánek R, Valent P, et al. Microelectr J 2009;40:595–7.
[3] Mitu B, Bauer-Gogonea S, Leonhartsberger H, Lindner M, Bauer S, Dinescu G. Plasma-deposited parylene-like thin films: process and material properties. Surf Coat Technol 2003;174–175:124–30.
[4] Miwa J, Suzuki Y, Kasagi N. J Microelectromech S 2008;17:611–22.
[5] Jeon BJ, Kim MH, Pyun JC. Sensor Actuat B: Chem 2011;154:89–95.
[6] Ledochowitsch, Félus RJ, Gibboni RR, Miyakawa A, Bao S and Maharbiz MM, MEMS 2011, Cancun, MEXICO. 2011;January:23–27,]
[7] Youn SW, Goto H, Takahashi M, Ogiwara M, Maeda R. Eng Mater 2007; 340–341:931–6.
[8] Noha Hong-Seok, Huang Yong, Hesketh Peter J. Sensors Actuators B 2004;102: 78–85.
[9] Kahouli A, Sylvestre A, Ortega L, Jomni F, Yangui B, Maillard M, et al. Appl Phys Lett 2009;94:152901.
[10] Jeffrey BF, Lu TM. Chemical vapor deposition the growth and properties of parylene thin films. Kluwer academic publishers; 2004.
[11] Senkevich JJ, Desu SB, Simkovic V. Polymer 2000;41:2379–90.
[12] You L, Yang G-R, Knorr DB, McDonalds JF, Lu T-M. Appl Phys Lett 1994;63: 2812–4.
[13] Lee SM. Kirk-Othmer encyclopedia of chemical technology. 3d ed., vol. 24. New York: John Wiley and Sons; 1983. 744.
[14] Senkevich JJ, Seshu BD. Polymer 1999;40:5751–9.
[15] Strel'tsov DR, Grigor'eva EI, Dmitryakov PV, Erina NA, Mailyan KA, Pebalk AV, et al. Polym Sci Ser A 2009;51:881–90.
[16] Senkevich JJ, Seshu BD. Thin solid films 1998;322:148–57.
[17] Beach WF. Xylylene polymers. Kirk-Othmer encyclopedia of chemical technology. 4th ed.; 1998. suppl.
[18] Kroschwitz JI, editor. Electrical and electronic properties of polymers: a state-of-the-art compendium. New York: John Wiley & Sons; 1988.